

## Rapid and Selective Detection of Proteins by Dual Trapping using Gold Nanoparticles functionalized with Peptide Aptamers

Maurice Retout<sup>a</sup>, Hennie Valkenier<sup>a</sup>, Eléonore Triffaux<sup>b</sup>, Thomas Doneux<sup>b</sup>, Kristin Bartik<sup>a</sup>, Gilles Bruylants<sup>a\*</sup>

a. *Engineering of Molecular Nanosystems, Université libre de Bruxelles (ULB), 50 Avenue F.D. Roosevelt, 1050 Bruxelles, Belgium.*

b. *Chimie Analytique et Chimie des Interfaces, Faculté des Sciences, Université libre de Bruxelles (ULB), Boulevard du Triomphe 2, CP 255, B-1050 Bruxelles, Belgium.*

\* E-mail: [gbruylan@ulb.ac.be](mailto:gbruylan@ulb.ac.be)

### Abstract

A colorimetric platform for the fast, simple and selective detection of proteins of medical interest is presented. Detection is based on the aggregation of two batches of peptide functionalized GNPs via the dual-trapping of the protein of interest. As proof of concept, we applied our platform to the detection of the oncoprotein Mdm2. The peptide aptamers used for the functionalization are based on the reported binding sequences of proteins p53 and p14 for the oncoprotein. Rapid aggregation, and a color change from red to purple, was observed upon addition of Mdm2 with concentrations as low as 20 nM. The selectivity of the system was demonstrated by the lack of response upon addition of BSA (in large excess) or of a truncated version of Mdm2, which lacks one of the peptide binding sites. A linear response was observed between 30 and 50 nM of Mdm2. The platform reported here is flexible and can be adapted for the detection of other proteins when two binding peptide aptamers can be identified. Unlike current immunoassay methods, it is a one-step and rapid method with an easy readout signal and low production costs.

KEYWORDS : gold nanoparticles, Mdm2, dual-trapping, peptide aptamer, nanosensor

Protein biomarkers are the major target for most current medical diagnostics.<sup>1-4</sup> The concentration of these proteins can potentially also provide information on the stage of the disease. Convenient, fast, cheap and sensitive protein-sensing methods, which can detect small variations in protein levels, are thus of great interest as they could lead to earlier diagnosis and to a better follow-up of pathological conditions.

The current gold-standard for protein detection is the enzyme-linked immunosorbent assay (ELISA).<sup>5</sup> Despite its high sensitivity this system possesses significant drawbacks, including high production costs, complex procedures and the need for trained operators, limiting its use in a point-of-care setting. Systems based on gold nanoparticles (GNPs) are, in this context gaining interest because GNPs have remarkable optical properties,<sup>6,7</sup> can be easily functionalized and are furthermore considered to be biocompatible.<sup>8</sup> They exhibit a localized

surface plasmon resonance (LSPR) band in the visible region, which can be exploited for colorimetric sensing as it is strongly dependent on the dielectric properties of the local environment (including solvent and adsorbates).<sup>9,10</sup> The most unambiguous signal is obtained with GNP aggregation, as this leads to coupling between the surface plasmon of neighboring nanoparticles and a significant change in the LSPR band.<sup>11,12</sup> Various GNP aggregation strategies have thus been developed for the detection of a wide range of analytes for biomedical diagnostics<sup>13,14</sup> and therapeutic applications.<sup>15,16</sup> The GNPs are for these applications almost always functionalized with antibodies,<sup>17</sup> which suffer from some severe and well-known drawbacks such as large molecular dimensions, stability issues, poor control of the orientation at the GNPs surface or large batch-to-batch variation.<sup>18-20</sup> To address these problems, synthetic affinity probes such as nucleic acid aptamers and, more recently, peptide aptamers have been considered for the detection of biomolecules. The term "peptide aptamer" has been originally coined to describe a "combinatorial protein molecule consisting of a variable peptidic sequence inserted within a constant scaffold protein"<sup>21</sup> although by extension the terminology is often applied to peptide affinity probes with good selectivity towards given targets. Peptides offer a promising alternative to antibodies, because they are far less expensive, easier to synthesize in a reproducible way, to manipulate and to graft onto GNPs following a well-controlled immobilization chemistry.

We present here a protein detection platform, which is based on the use of peptide functionalized GNPs that could fit the requirements for a point-of-care system. This platform exploits a double recognition strategy using two sets of GNPs, each functionalized with a different peptide. The two peptides are able to recognize the target protein simultaneously, and the formation of the ternary complex induces the aggregation of the GNPs (Fig. 1). High selectivity is ensured by the dual-trapping mechanism and, in combination with the easy read-out of GNP aggregation, the simplicity of use and its relatively low-cost, this system is a good candidate for a point-of-care device. As a proof of concept, the detection of the oncoprotein Mdm2 is demonstrated.

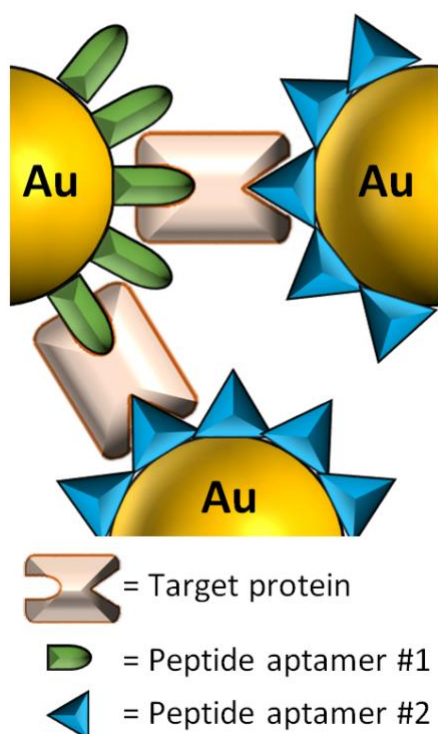


**Fig. 1** Schematic representation of the detection of a target protein with GNPs functionalized with different peptide aptamers, each recognizing a specific site of the protein.

Mdm2 (491 a.a.) is considered to be the main negative regulator of the tumor suppressor protein p53, which is commonly called the “cellular gatekeeper for growth and division” due to its critical role in the response following a cellular stress.<sup>22,23</sup> It has been brought to light that in more than 7% of human tumor cells, Mdm2 is strongly overexpressed (e.g. 10-fold in leukemia)<sup>24</sup>, and that this percentage increases to 20 % in soft tissue tumors.<sup>25</sup> The early detection of abnormal levels of Mdm2 is consequently seen as a promising diagnostic target for certain cancers.

## Results and Discussion

Citrate protected GNPs with a narrow size distribution were synthesized following a modified Turkevich method.<sup>26</sup> The colloids were dialyzed against 0.1 mM citrate solutions just after synthesis. TEM measurements revealed an average diameter of 15.6 nm for the nanoparticles, and the colloidal suspension exhibited a sharp LSPR band with a  $\lambda_{\max}$  at 521 nm (Fig. S1). A hydrodynamic radius of 30 nm was determined by dynamic light scattering (DLS).

The peptides used to functionalize the two sets of GNPs were derived from the binding sequences of proteins p53 and p14, which can naturally form a ternary complex with Mdm2.<sup>27</sup> While p53 is negatively regulated by Mdm2, p14 is an inhibitor of this regulation and restores the function of p53.<sup>28</sup> The minimal sequences of these two proteins involved in the recognition, as reported in the literature,<sup>29–31</sup> were used to design the peptide aptamers (Fig. 2). In both cases, additional residues from the natural sequence were kept to add some flexibility in the construct, and two cysteine residues were added at the N-term and C-term

extremities of the p53 and p14 peptides, respectively, to enable the grafting on the GNPs (Fig. 2).

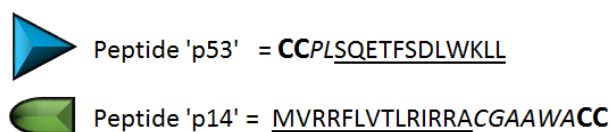


**Fig. 2** Amino acid sequences of peptide-p53 and peptide-p14 aptamers which were grafted on the GNPs; the recognition sequence is underlined and the flexibility part is in italic.

The p53-peptide, which is negatively charged, was grafted on the GNPs using a simple one-step protocol with an excess of peptide (GNP-p53). A red shift of the LSPR band by 2.5 nm (Fig. S2) and an increase of the hydrodynamic radius of the particles of 30 % were observed. After centrifugation, the fluorescence emission of the tryptophan residue of the free peptide in the supernatant was measured in order to quantify the level of grafting. The grafting density was furthermore verified by detaching the peptides from the purified GNPs using dithiothreitol (DTT) and measuring the fluorescence in the supernatant after centrifugation. A good agreement was obtained between these two quantification methods (Table S1) and the grafting level was estimated to be around  $450 \pm 100$  peptides per GNP, corresponding to a grafting density of 0.50 peptide/nm<sup>2</sup>.

The second aptamer, peptide-p14, is positively charged and it was not possible to reach the same grafting level as the immobilization of a positively charged peptide on citrate protected GNPs (which present a global negative zeta potential) cancels the surface potential and destabilizes the colloidal suspension. A stable colloidal suspension of GNP-p14 was obtained with around 50 peptides per GNP. The grafting was confirmed by the small red shift of the LSPR band ( $\Delta\lambda_{\text{max}} = 1.0$  nm, Fig. S3) and an increase of the hydrodynamic radius of approximately 23 %.

Mixing the two batches of functionalized nanoparticles, GNP-p53 and GNP-p14, at equal GNP concentrations (1 nM total concentration) gave rise to a stable solution. The addition of Mdm2 (50 nM) led to a clear color change with a rapid increase of the absorbance at 680 nm and decrease of the absorbance at 523 nm (Fig. 3), which is a clear signature of GNP aggregation. This was confirmed by the comparison of TEM pictures of GNP-p53/GNP-p14 mixture deposits before and 20 minutes after the addition of Mdm2 (Fig. S6). The particles show a clear tendency to form large aggregates in the presence of Mdm2, which is not the case in the absence of the protein. The compact aggregates are a signature of a reaction limited colloidal aggregation mode (RLCA).<sup>32,33</sup> It is worth mentioning that the kinetics of the aggregation is in agreement with previously observed protein induced aggregation of GNPs of similar size.<sup>34</sup>

To verify that the aggregation was indeed due to the selective binding of Mdm2 to the two sets of peptide-functionalized GNPs and the formation of the ternary complex, various control experiments were run. No aggregation was observed when Mdm2 was added either to a

suspension of GNP-p53, or a suspension of GNP-p14. The addition of Bovine Serum Albumin (BSA) to the GNP-p53/GNP-p14 suspension also did not induce any aggregation, even at its physiological concentration (600  $\mu\text{M}$ ). BSA has a size and charge similar to that of Mdm2 and is known to easily adsorb onto surfaces. To highlight the need for the double recognition, a truncated version of Mdm2 (deletion of residues 1-200) that does not possess the N-terminal hydrophobic pocket required to bind p53, was also tested. Once again, no shift of the LSPR band is observed, only a rapid and small increase of the overall absorption resulting from the increased turbidity of the sample. In all cases the  $A_{680}/A_{523}$  ratio does not evolve with time, which is a clear indication that aggregation does not occur (Fig 3c and Fig. S3-S5).

To show the robustness of the system, the detection of Mdm2 (50 nM) was tested in the presence of a large excess of BSA (50  $\mu\text{M}$ ). An unambiguous aggregation signal was rapidly observed (Fig. 3c and Fig. S7). The detection capacity of the platform was also tested using different Mdm2 concentrations, ranging between 20 and 80 nM (Fig. 4 and S8), a concentration range that encompasses the normal biological concentration in Mdm2.<sup>35</sup> The ratio of the absorbance of the LSPR band at 680 nm to that at 523 nm after 20 minutes was measured. A linear relation was obtained between 30 and 50 nM ( $R^2 = 0.993$ , Fig. 4 and Fig. S8), showing the potential of this system to function as quantitative colorimetric sensor. The presence of Mdm2 could however be evidenced at all tested concentrations but below 30 nM, the aggregation process is slow and above 50 nM the system starts to saturate. For very high concentrations of Mdm2 (80 nM), the protein-to-GNP ratio is so large that the GNP surface is saturated with protein, hindering the formation of the ternary complexes. This saturation effect was confirmed by a simple experiment, wherein the concentration of GNPs was decreased. As expected for a saturation phenomenon, the same trend in the  $A_{680}/A_{523}$  ratio was observed but at lower concentrations in Mdm2. The linear relationship observed for the  $A_{680}/A_{523}$  ratio as a function of protein concentration definitely paves the way to the development of a quantitative detection assay. Efforts are ongoing to determine the optimal GNP concentration and peptide grafting levels to extend the accessible Mdm2 concentration range.

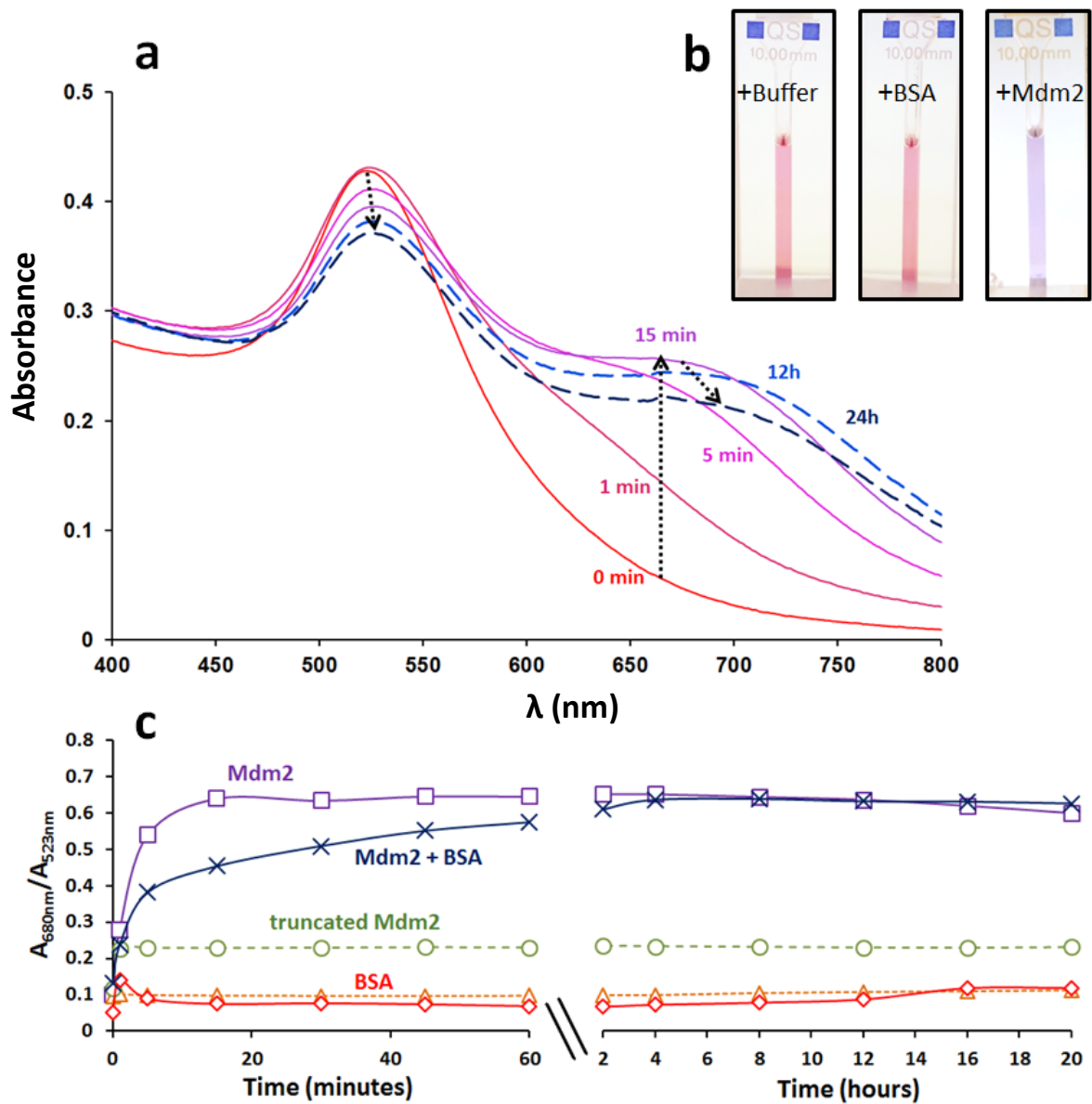


**Fig. 3** (a) Time resolved UV-vis spectra of the GNP-p53 / GNP-p14 suspension in the presence of Mdm2 (50 nM); (b) GNP-p53 / GNP-p14 suspension 20 minutes after addition of Tris-HCl buffer (left) of 50 nM BSA (middle) or 50 nM Mdm2 (right); (c) Evolution of the ratio  $A_{680}/A_{523}$  from 0 to 60 minutes (left) and from 2 to 20 hours (right) in the presence of 50 nM Mdm2 ( $\square$ ), 50 nM truncated Mdm2 ( $\circ$ ), 50 nM Mdm2 with 50  $\mu\text{M}$  BSA ( $\times$ ), 50 nM BSA ( $\Delta$ ) or 600  $\mu\text{M}$  BSA ( $\diamond$ ).

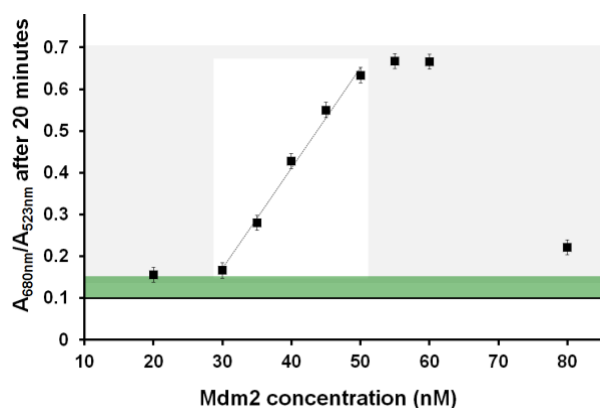


**Fig. 4**  $A_{680nm}/A_{523nm}$  after 20 minutes as a function of the Mdm2 concentration added to a GNP-p53/GNP-p14 suspension. The dotted line shows the linear relationship. The horizontal line represents the  $A_{680nm}/A_{523nm}$  ratio in the absence of protein and the green area represents the non-specific background (3 sigma calculated on 13 repetitions of the initial measurement in the absence of protein).

## Conclusion

We combined the capacity of peptide aptamers to selectively bind to a target protein with the optical properties of GNPs to build a rapid and robust colorimetric assay for the detection of the oncoprotein Mdm2. Our experiments show that GNP aggregation in the presence of Mdm2 results in a rapid and selective detection method for this protein, with an easily discernable signal already appearing after less than five minutes at concentrations as low as 20 nM. The developed strategy combines the concept of GNP aggregation induced by double recognition of the target protein by two distinct sets of functionalized nanoparticles with the use of an emerging class of recognition elements, peptide aptamers. Our results demonstrate that peptides can be efficiently used for a recognition process, replacing the more commonly used antibodies. Mdm2 was used as proof of concept for this strategy due to its strong biomedical interest, but similar peptide-based dual-trapping recognition assays could be developed for numerous other proteins of interest, for which peptide affinity probes can be identified among their natural partners/inhibitors. The properties of this platform - high selectivity, easy readout, efficiency of set-up, low cost - correspond perfectly with point-of-care expectations and this evolution is envisaged.

## Acknowledgements

The authors thank the 4MAT and the Pharmaceutics and Biopharmaceutics laboratories of the ULB for access to their TEM and DLS, respectively. This research was funded by the *Actions de Recherches Concertées* of the *Fédération Wallonie-Bruxelles* and the *Fondation Van Buuren*. MR thanks the *Ecole polytechnique de Bruxelles* for funding. Th.D. gratefully acknowledges the financial support from the Fonds National de la Recherche Scientifique (F.R.S.-FNRS).

## Supporting information

Supporting Information Available: The following file is available free of charge. PDF containing the materials and methods section, additional figures containing UV-vis spectra of the various GNP suspensions (functionalized or not), the UV-vis spectra as function of time of the detection tests (with Mdm2 at concentration ranging from 20 to 80 nM, BSA, truncated version of Mdm2, mixture of Mdm2 and BSA), table showing the grafting levels of the p53-peptide on the GNPs, and TEM images.

## References

- (1) Daniels, M. J. Abnormal Cytokinesis in Cells Deficient in the Breast Cancer Susceptibility Protein BRCA2. *Science* **2004**, *306*, 876–879.
- (2) Bai, V. U.; Kaseb, A.; Tejawani, S.; Divine, G. W.; Barrack, E. R.; Menon, M.; Pardee, A. B.; and Reddy, G. P.-V. Identification of prostate cancer mRNA markers by averaged differential expression and their detection in biopsies, blood, and urine. *Proc. Natl. Acad. Sci. U. S. A.* **2007**, *104*, 2343–2348.
- (3) Masson, J. F.; Battaglia, T. M.; Khairallah, P., Beaudoin, S., and Booksh, K. S. Quantitative measurement of cardiac markers in undiluted serum. *Anal Chem* **2007**, *79*, 612–619.
- (4) Nielsen, S. L.; Andersen, P. L.; Koch, C.; Jensenius, J. C.; Thiel, S. The level of the serum opsonin, mannan-binding protein in HIV-1 antibody-positive patients. *Clin. Exp. Immunol.* **1995**, *100*, 219–222.
- (5) Haab, B. B. Applications of antibody array platforms. *Curr. Opin. Biotechnol.* **2006**, *17*, 415–421.
- (6) Hutter, E.; Fendler, J. H. H. Exploitation of localized surface plasmon resonance. *Adv. Mater.* **2004**, *16*, 1685–1706.
- (7) Kelly, K. L.; Coronado, E.; Zhao, L. L.; Schatz, G. C. The optical properties of metal nanoparticles : the influence of size, shape, and Dielectric Environment. *J. Phys. Chem. B* **2003**, *107*, 668–677.
- (8) Shukla, R.; Bansal, V.; Chaudhary, M.; Basu, A.; Bhonde, R. R.; Sastry, M. Biocompatibility of gold nanoparticles and their endocytotic fate inside the cellular compartment: A microscopic overview. *Langmuir* **2005**, *21*, 10644–10654.
- (9) Link, S.; El-sayed, M. A. Spectral Properties and Relaxation Dynamics of Surface Plasmon Electronic Oscillations in Gold and Silver Nanodots and Nanorods. *J. Phys. Chem. B* **1999**, *103*, 8410–8426.
- (10) Jain, P. K.; Huang, X.; El-Sayed, I. H.; El-Sayed, M. a. Review of some interesting surface plasmon resonance-enhanced properties of noble metal nanoparticles and their applications to biosystems. *Plasmonics* **2007**, *2*, 107–118.
- (11) Elghanian, R.; Storhoff, J. J.; Mucic, R. C.; Letsinger, R. L.; Mirkin, C. A. Selective colorimetric detection of polynucleotides based on the distance-dependent optical properties of gold nanoparticles. *Science* **1997**, *277*, 1078–1081.



- (12) Ghosh, S. K.; Pal, T. Interparticle coupling effect on the surface plasmon resonance of gold nanoparticles: from theory to applications. *Chem. Rev.* **2007**, *107*, 4797–862.
- (13) Zhou, W.; Gao, X.; Liu, D.; Chen, X. Gold Nanoparticles for in Vitro Diagnostics. *Chem. Rev.* **2015**, *115*, 10575–10636.
- (14) Saha, K.; Agasti, S. S.; Kim, C.; Li, X.; Rotello, V. M. Gold nanoparticles in chemical and biological sensing. *Chem. Rev.* **2012**, *112*, 2739–2779.
- (15) Huang, X.; El-Sayed, I. H.; Qian, W.; El-Sayed, M. A. Cancer cell imaging and photothermal therapy in the near-infrared region by using gold nanorods. *J. Am. Chem. Soc.* **2006**, *128*, 2115–2120.
- (16) Nam, J.; Won, N.; Jin, H.; Chung, H.; Kim, S. pH-induced aggregation of gold nanoparticles for photothermal cancer therapy. *J. Am. Chem. Soc.* **2009**, *131*, 13639–13645.
- (17) Lesniewski, A.; Los, M.; Jonsson-Niedziolka, M.; Krajewska, A.; Szot, K.; Los, J. M.; Niedziolka-Jonsson, J. Antibody modified gold nanoparticles for fast and selective, colorimetric T7 bacteriophage detection. *Bioconjug. Chem.* **2014**, *25*, 644–648.
- (18) Kim, B.; Choi, S.; Han, S.; Choi, K.-Y.; Lim, Y. Stabilization of  $\alpha$ -helices by the self-assembly of macrocyclic peptides on the surface of gold nanoparticles for molecular recognition. *Chem. Commun.* **2013**, *49*, 7617–7619.
- (19) Chang, C.-C.; Chen, C.-P.; Lee, C.-H.; Chen, C.-Y.; Lin, C.-W. Colorimetric detection of human chorionic gonadotropin using catalytic gold nanoparticles and a peptide aptamer. *Chem. Commun.* **2014**, *50*, 14443–14446.
- (20) Lai, H.-Z.; Wang, S.-G.; Wu, C.-Y.; Chen, Y.-C. Detection of *Staphylococcus aureus* by Functional Gold Nanoparticle-Based Affinity Surface-Assisted Laser Desorption/Ionization Mass Spectrometry. *Anal. Chem.* **2015**, *87*, 2114–2120.
- (21) Baines, I. C.; Colas, P. Peptide aptamers as guides for small-molecule drug discovery. *Drug Discov. Today* **2006**, *11*, 334–341.
- (22) Wu, X.; Bayle, J. H.; Olson, D.; Levine, A. J. The p53-mdm-2 autoregulatory feedback loop. *Genes Dev.* **1993**, *53*, 1126–1132.
- (23) Levine, A. J. P53, the Cellular Gatekeeper for Growth and Division. *Cell* **1997**, *88*, 323–331.
- (24) Zhou, M.; Gu, L.; Abshire, T. C.; Homans, A.; Billett, A. L.; Yeager, A. M.; Findley, H. W. Incidence and prognostic significance of MDM2 oncoprotein overexpression in relapsed childhood acute lymphoblastic leukemia. *Leukemia* **2000**, *14*, 61–67.
- (25) Momand, J.; Jung, D.; Wilczynski, S.; Niland, J. The MDM2 gene amplification database. *Nucleic Acids Res.* **1998**, *26*, 3453–3459.
- (26) Doyen, M.; Bartik, K.; Bruylants, G. UV-Vis and NMR study of the formation of gold nanoparticles by citrate reduction: observation of gold-citrate aggregates. *J. Colloid Interface Sci.* **2013**, *399*, 1–5.
- (27) Savchenko, A.; Yurchenko, M.; Snopok, B.; Kashuba, E. Study on the spatial architecture of p53, MDM2, and p14ARF containing complexes. *Mol. Biotechnol.* **2009**, *41*, 270–277.

- (28) Lohrum, M. A.; Ashcroft, M.; Kubbutat, M. H.; Vousden, K. H. Contribution of two independent MDM2-binding domains in p14(ARF) to p53 stabilization. *Curr. Biol.* **2000**, *10*, 539–542.
- (29) Baek, S.; Kutchukian, P. S.; Verdine, G. L.; Huber, R.; Holak, T. A.; Lee, K. W.; Popowicz, G. M. Structure of the stapled p53 peptide bound to Mdm2. *J. Am. Chem. Soc.* **2012**, *134*, 103–106.
- (30) Vousden, K. H.; Lu, X. Live or let die: the cell's response to p53. *Nat. Rev. Cancer* **2002**, *2*, 594–604.
- (31) Weber, J. D.; Kuo, M.; Bothner, B.; Enrico, L.; Kriwacki, R. W.; Roussel, M. F.; Sherr, C. J.; Giammarino, E. L. D. I. Cooperative Signals Governing ARF-Mdm2 Interaction and Nucleolar Localization of the Complex. *Mol. Cell. Biol.* **2000**, *20*, 2517–2528.
- (32) Lin, M. Y.; Lindsay, H. M.; Weitz, D. A.; Ball, R. C.; Klein, R.; Meakin, P. Universality in colloid aggregation. *Nature* **1989**, *339*, 360–362.
- (33) Doyen, M.; Goole, J.; Bartik, K.; Bruylants, G. Amino acid induced fractal aggregation of gold nanoparticles: Why and how. *J. Colloid Interface Sci.* **2016**, *464*, 60–166.
- (34) Huang, C.-C.; Huang, Y.-F.; Cao, Z.; Tan, W.; Chang, H.-T. Aptamer-modified gold nanoparticles for colorimetric determination of platelet-derived growth factors and their receptors. *Anal. Chem.* **2005**, *77*, 5735–5741.
- (35) Wang, Y. V.; Wade, M.; Wong, E.; Li, Y.-C.; Rodewald, L. W.; Wahl, G. M. Quantitative analyses reveal the importance of regulated Hdmx degradation for p53 activation. *Proc. Natl. Acad. Sci. U. S. A.* **2007**, *104*, 12365–12370.

